

Modeling electron-electron interactions in reduced-dimensional materials: Bond-charge Coulomb repulsion and dimerization in Peierls-Hubbard models

D. K. Campbell, J. Tinka Gammel, and E. Y. Loh, Jr.

Center for Nonlinear Studies and Theoretical Division, Los Alamos National Laboratory, Los Alamos, New Mexico 87545

(Received 30 January 1990; revised manuscript received 7 March 1990)

To the conventional Peierls-Hubbard model, involving both on-site (U) and nearest-neighbor (V) Coulomb repulsions, we add "off-diagonal" terms, not expressible purely in terms of site densities, representing bond-bond (W) and mixed bond-site (X) electron-electron repulsive interactions involving nearest neighbors. We review earlier analyses of these interactions and discuss relative magnitudes of the parameters in applications to real materials. As a specific illustration, we investigate the effects of the off-diagonal W and X terms on dimerization in the one-dimensional, half-filled-band Peierls-Hubbard models, which have been widely applied to conjugated polymers (such as trans-polyacetylene) and to related quasi-one-dimensional charge-density wave (CDW) systems. Using both weak- and strong-coupling perturbation theory for large systems and exact diagonalizations of small systems, we investigate thoroughly the nature of the ground state of the model. For a broad range of the site-diagonal Hubbard parameters (U, V), including the values believed to be relevant to trans-polyacetylene, we find that the off-diagonal terms (W, X) initially *enhance* dimerization, thereby stabilizing the dimerized [or bond-order-wave (BOW)] ground state. For (unphysically) large values of W relative to U and V , dimerization is destroyed, and the BOW ground state goes over to a ferromagnetic ground state or a CDW ground state, depending on the relative sizes of U, V , and W . We conclude with a general discussion of the applicability of the Peierls-Hubbard models to quasi-one-dimensional materials, including the potential importance of the breaking of charge conjugation ("particle-hole") symmetry by the X term.

I. INTRODUCTION

The role of electron-electron ($e-e$) interactions in solid-state systems continues to be the subject of intense investigation and debate. Much of the recent discussion has been stimulated by experimental work on exciting novel materials, including high-temperature superconducting copper oxides, "heavy-fermion" systems, organic synthetic metals, and halogen-bridged transition-metal chains. Unlike conventional metals, for which standard single-electron (band) theories describe quantitatively the electronic structures and excitations, these new "correlated" materials are thought to have properties strongly influenced or even dominated by many-body effects arising from strong $e-e$ interactions. Indeed, most current theoretical models of the high- T_c materials are predicated on the dominance of strong Coulomb interactions. Similarly, in the synthetic metals, a class of organic electronic materials which subsumes conducting polymers and a variety of charge-transfer salts including superconductors, models involving direct $e-e$ effects are becoming increasingly common.

In the area of conducting polymers, the debate between advocates of single-electron approaches and those supporting many-body theories has been particularly long standing. Consider the case of polyacetylene— $(\text{CH})_x$ —the quasi-one-dimensional conjugated polymer that, in the theorist's idealized world, corresponds to the infinite limit of the finite polyenes, $\text{C}_{2n}\text{H}_{2n+2}$. In the chemical literature the existence of bond alternation ("dimeriza-

tion"), the origin of the optical gap, and the nature of the electronic excitations in conjugated π -electron systems like the finite polyenes have been debated for over fifty years.^{1,2} On one side are the Hückel single-electron theories,³ in which the optical gap is due entirely to the bond alternation or dimerization that exists because of the coupling of nuclear and electronic motions. On the other side are the Pariser-Parr-Pople (PPP) models,⁴ which fit very accurately the observed electronic excitations (both the optical gap and optically forbidden transitions) in finite polyenes⁵ by assuming that $e-e$ effects dominate and that bond alternation is a secondary effect. In the physics literature, the same debate has been couched in terms of electron-phonon (e -ph) versus $e-e$ interactions. The standard physicists' single-electron approach to $(\text{CH})_x$ —the celebrated Su-Schrieffer-Heeger (SSH) model⁶—can be viewed as one of the class of Peierls models in which e -ph interactions dominate and the optical gap is linked directly to the bond alternation. In contrast, the Hubbard models⁷ applied to $(\text{CH})_x$ (Refs. 2, 8–15) treat the limit of dominant $e-e$ interactions and assume that the polymer is essentially a Mott-Hubbard insulator with ancillary e -ph interactions.

In fact, experimental results in finite polyenes and polyacetylene indicate that *both* e - p and e - e interactions play important roles, with some observables affected more by the former, and some by the latter, interactions.² To go beyond this qualitative statement it is essential to have tractable models that capture the essence of both e - p

and e - e interactions and that represent faithfully their combined, or competing, effects. This is clearly the case not only for conducting polymers but also for the entire class of novel materials; for example, in the high- T_c superconducting oxides the relation between structural changes (tetragonal to orthorhombic transitions), "breathing modes," and electronic properties must be modeled correctly before the materials can be understood fully.

For conjugated polymers, the extended Peierls-Hubbard or PPP-plus-phonon models have been widely accepted as examples of theories correctly incorporating the effects of both e -ph and e - e interactions. Considerable effort has gone into obtaining perturbative,¹⁰ mean-field,¹² and true many-body^{2,8,9,11,13-15} solutions to these models. Recently, however, fundamental objections have been raised¹⁶ to the very manner in which these theories model e - e interactions. The crucial objection is that both the PPP and Hubbard models incorporate only (lattice) *site-diagonal* parts of the e - e interactions. Since, however, the Coulomb potential between two electrons depends only on the distance between them and is thus translationally invariant, independent of the underlying nuclear lattice, a first-principles theory *must* also contain terms that are *not* diagonal in a site representation. To exemplify this rediscovery (by physicists) of the "off-diagonal" terms in the Coulomb interaction when it is represented in terms of the Wannier functions appropriate to tight-binding models, we again consider the specific case of polyacetylene. If $\phi_j(r)$ is the Wannier function localized around the j th (CH) unit, then the *general* e - e interaction matrix element has the form^{7,16}

$$\begin{aligned} \langle ij|V_{e-e}|kl\rangle \\ \equiv \int \int dr dr' \phi_i^*(r)\phi_j^*(r')V_{e-e}(r-r')\phi_k(r)\phi_l(r') . \end{aligned} \quad (1.1)$$

For $i=k$ and $j=l$, these matrix elements involve only on-site densities: For example, for $i=j=k=l$, the matrix element is proportional to the on-site Hubbard U (Ref. 7) and for $i=k, j=l=i+1$, the matrix element is proportional to the nearest-neighbor Hubbard V .⁷ For other combinations of i, j, k, l , off-diagonal terms arise. Specifically, the two such terms involving only nearest neighbors are

$$2W \equiv \langle i, i+1|V_{e-e}|i+1, i\rangle \quad (1.2a)$$

and

$$X \equiv \langle i, i+1|V_{e-e}|i, i\rangle . \quad (1.2b)$$

Physically, $W(>0)$, which is in fact just the standard (Fock) exchange term between neighboring Wannier orbitals, corresponds to the Coulomb repulsion between electrons "localized" on the *bond* between sites i and $i+1$. In contrast, X is a mixed bond-site term and is often referred to as a density-dependent hopping;¹⁷ as we shall later show, it has the important characteristic that it breaks the particle-hole symmetry of the standard Hubbard model.

In a second quantized approach, the W and X terms take the forms

$$H_W^{(\text{int})} \equiv W \sum_l B_{l,l+1} B_{l,l+1} , \quad (1.3a)$$

and

$$H_X^{(\text{int})} = X \sum_l B_{l,l+1} (n_l + n_{l+1}) . \quad (1.3b)$$

Here the (Hermitian, nearest-neighbor) bond-charge operator $B_{l,l+1}$ is defined by

$$B_{l,l+1} \equiv \sum_{\sigma} c_{l,\sigma}^{\dagger} c_{l+1,\sigma} + c_{l+1,\sigma}^{\dagger} c_{l,\sigma} \quad (1.4a)$$

and the on-site charge density is

$$n_l \equiv \sum_{\sigma} c_{l,\sigma}^{\dagger} c_{l,\sigma} . \quad (1.4b)$$

In (1.4), $c_{i\sigma}$ annihilates an electron with spin σ in the Wannier orbital at site l . From (1.3) and (1.4) one sees explicitly the fact noted above that these "bond-charge-bond-charge" (W) and mixed "bond-charge-site-charge" (X) repulsions are *not* diagonal in a site representation and hence are *not* incorporated in the standard PPP or extended Hubbard models.

In the specific context of $(\text{CH})_x$, the potential importance of this omission is readily recognized. In the absence of e - e interactions, the ground state of $(\text{CH})_x$ is (in the physical terminology) the $2k_F$ bond-order-wave (BOW) predicted by Peierls theorem, which (in chemical terms) corresponds to an alternating pattern of single (long) and double (short) bonds. Since there is one π -electron per site, the band is half filled and the $2k_F$ instability produces the dimerization-bond-alternation pattern indicated in Fig. 1; the chemical double bonds are physically shorter than the single bonds by roughly 0.1 Å.¹⁸ If one includes e - e interaction effects via the standard Hubbard model, one finds unambiguously [using exact (numerical) many-body methods] that (for the expected range of e -ph couplings) the on-site Coulomb repulsion actually *enhances* dimerization up to fairly large values ($U > 6t_0$) (Refs. 13-15) and that dimerization persists for all finite U , with the results for the Peierls-Hubbard model smoothly joining those obtained for the spin-Peierls model at very large U .^{11,19} Further, a nearest-neighbor diagonal repulsion (V) enhances dimerization still more (for $V < U/2$).¹⁵ Although in addition to these exact numerical studies one can provide an appealing explanation

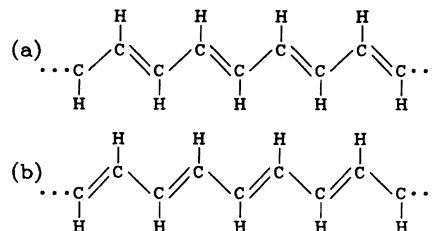


FIG. 1. A schematic illustration of bond alternation-dimerization in $\text{trans}(\text{CH})_x$.

of this phenomenon using “barrier to resonance” arguments,⁸ these results are still widely regarded as counter to the conventional wisdom that Coulomb interactions should suppress the buildup of charge *anywhere*, on the sites or on the bonds. On the basis of this intuition, the bond-bond repulsion would seem to suppress dimerization, since it opposes the buildup of charge on the bonds. Thus, the *absence* of W and X in the standard extended Peierls-Hubbard models suggests *a priori* that these models may *artificially* favor the continuation of dimerization in the half-filled band into the region of intermediate to strong Coulomb interaction.

More generally, the omission of terms such as W and X raises significant questions about the appropriateness of Hubbard or PPP-like models for describing e - e interactions in the whole class of novel solid-state materials. In fact, it has been proposed that the X and W terms are the mechanisms driving superconductivity²⁰ and ferromagnetism,²¹ respectively.²² In view of the very wide-spread application of these models, this issue is obviously important and must be investigated in a thorough and definitive manner. In the ensuing article, we examine carefully several aspects of this problem, focusing on the effect of W and X on dimerization in the half-filled band. Our results will speak directly to the issue of the applicability of these models.

Perhaps the first general comment that should be made in the context of the off-diagonal e - e interaction terms is that their existence has long been recognized. In the original derivations⁴ of the PPP models for π -electron motion in finite polyenes, these terms were discussed and their magnitudes estimated. Their exclusion—the “zero differential overlap” approximation⁴—in the model was justified by earlier (essentially exact) studies of benzene²³ and was examined further in a number of later papers.¹ In addition, in his original studies⁷ of e - e interaction effects in the narrow bands characteristic of transition metals, Hubbard discussed these off-diagonal terms and, on the basis of specific estimates, concluded that they were small compared to the on-site terms and could safely be neglected. Taken together these chemical and physical studies do suggest that Peierls-Hubbard models are a reasonable point of departure for studying the effects of e - e interaction in conduction polymers and related novel materials. However, to understand in detail the potential effects of W , X , and related terms in these systems, it is necessary to solve exactly a model including these terms and to compare this solution with that of the conventional Peierls-Hubbard models.

In the case of the specific question of the effect of W and X on dimerization in the half-filled band, the early quantitative analyses were limited to first-order, weak-coupling perturbation theory¹⁶ and to variational methods.²⁴ More recently, studies using both exact-valence-bond methods²⁵ and “g-ology” arguments,²⁶ have further clarified several aspects of the potential effects of the W and X terms. In the present article (briefer, less-detailed versions of which have appeared previously²⁷), we extend these analyses, treating both weak- and strong-coupling perturbation theory consistently to second order and performing exact diagonalizations on

finite-size systems which are sufficiently large to reflect the true behavior of the models. From these different approaches we obtain a fully consistent picture of the nature of the ground state in the quasi-one-dimensional half-filled band with both diagonal and off-diagonal e - e interactions. Whereas the previous first-order perturbation-theory results (applicable only for U, V, X, W, \dots all small and comparable) suggest that W suppresses dimerization monotonically, for typical expected values of the on-site parameters U and V the dimerization does not decrease but rather holds up well as W is increased before dropping discontinuously to zero in a ferromagnetic phase for $W > W_c$. Indeed, for the intermediate coupling range $U \sim 4t_0$ and $V < U/2$, the dimerization initially *increases* with W and, for the values of (U, V, X, W, \dots) thought to be relevant to $(\text{CH})_x$, dimerization is typically *enhanced* over its value at $W=0$. An argument supporting this seemingly counter-intuitive result is given below in our treatment of the strong-coupling limit.

To present our results cogently, we have organized the remainder of the article into four sections. In Sec. II we introduce the model Hamiltonian, including both e -ph and e - e interactions, both diagonal and off-diagonal, up to nearest neighbors. These terms include U , V , X , and W . We illustrate directly, using a (partially solvable) one-dimensional Kronig-Penny band-theory model plus screened Coulomb interaction, that the e - e interaction parameters cannot be assigned arbitrary values but must be determined consistently. Except for the case of extreme screening, we find $U > V > X > W$, consistent with earlier estimates in benzene²³ and in the $3d$ transition metals.⁷ In Sec. III, we explore first weak-coupling perturbation theory and then examine two distinct but related strong-coupling expansions. Section IV contains our exact-diagonalization calculations. We find that the analytic results from a dimer calculation reflect many of the qualitative features of, and provide useful insight into, our exact results on 4, 6, 8, and 10 site rings. The convergence of these results indicates that, at least for determining the phase diagram describing the ground state, it is unnecessary to go to systems of larger size. Section V contains our conclusions and a discussion of their relevance for real materials. The two appendices present technical details of our weak-coupling perturbation-theory calculations and our numerical scheme for exact diagonalization.

II. A PEIERLS-HUBBARD MODEL WITH OFF-DIAGONAL COULOMB INTERACTIONS

A. Hamiltonian

To analyze the effects of off-diagonal Coulomb terms in quasi-one-dimensional systems, we consider the modified Peierls-Hubbard Hamiltonian

$$\begin{aligned}
 H = & - \sum_l (t_0 - \alpha \delta_l) B_{l,l+1} + \frac{1}{2} K \sum_l \delta_l^2 + \frac{1}{2} M \sum_l v_l^2 \\
 & + U \sum_l n_{l\uparrow} n_{l\downarrow} + V \sum_l n_l n_{l+1} + X \sum_l B_{l,l+1} (n_l + n_{l+1}) \\
 & + W \sum_l (B_{l,l+1})^2, \tag{2.1}
 \end{aligned}$$

where, the operators in (2.1) have been defined in Sec. I. In H , t_0 is the hopping integral for the uniform lattice, α is the e -ph coupling, δ_l is the relative displacement between the ions at sites l and $l+1$, K represents the cost of distorting the lattice, and M is the mass of the (CH) unit at site l with velocity v_l . As we do not expect quantum phonons to be important for realistic values of M , for most of our discussion we consider only the $M \rightarrow \infty$ (adiabatic) limit, where $v_l \equiv 0$. We briefly discuss the anti-adiabatic limit in Sec. III C. Finally, U , V , X , and W model the e - e interactions. As discussed above, U represents the on-site Coulomb repulsion, V the nearest-neighbor repulsion, X is the "mixed" term involving both site-charge and bond-charge repulsive effects, and W is the pure bond-charge-bond-charge repulsion.

In restricting our considerations to U , V , X , and W , we have ignored longer-range, many-body terms corresponding to matrix elements in (1.1) in which differences in the indices are greater than one. We have chosen this restricted model both to limit the number of parameters and to permit ready comparison of its results, which incorporate off-diagonal effects, with the results of the well-studied Peierls-extended Hubbard^{2,8-15} models.

For $U = V = W = X = 0$, this model reduces to the SSH Hamiltonian,⁶ in the (adiabatic) limit of classical ion displacements. Consistent with Peierls theorem, the ground state is a $2k_F$ BOW. In the half-filled band, this is a dimerized or bond-alternated ground state, which in the case of trans-(CH)_x produces the structure shown in Fig. 1. For $W = X = 0$, this Hamiltonian is the conventional extended Peierls-Hubbard^{2,8-15} model that has widely been used to model conducting polymers and in particular to investigate the competition between e -ph and e - e interactions in these systems. When both W and X are included, the model represents the effects of all Coulomb interactions—both on- and off-diagonal—up to and including nearest-neighbor matrix elements.

In terms of the Coulomb potential $V_{e-e}(x)$ and the Wannier functions $\phi_n(x) \equiv \phi(x - na)$ —which, since we are considering a single-band model, we can assume to be real—the interaction constants in (2.1) can be expressed as

$$U = \int dx dx' \phi^2(x) V_{e-e}(x - x') \phi^2(x'), \quad (2.2a)$$

$$V = \int dx dx' \phi^2(x) V_{e-e}(x - x') \phi^2(x' - a), \quad (2.2b)$$

$$X = \int dx dx' \phi^2(x) V_{e-e}(x - x') \phi(x') \phi(x' - a), \quad (2.2c)$$

and

$$2W = \int dx dx' \phi(x) \phi(x - a) V_{e-e}(x - x') \phi(x') \phi(x' - a). \quad (2.2d)$$

B. Values of the parameters

Since all the e - e interaction parameters in (2.1) and (2.2) arise from the Coulomb potential, they cannot be assigned arbitrary values but must be determined consistently. In the case of d bands in transition metals, Hubbard⁷ has estimated $U \sim 20$ eV, $V \sim 6$ eV, $X \sim \frac{1}{2}$ eV,

and $W \sim \frac{1}{80}$ eV. In the case of finite polyenes, this determination has been carried out in detail for (isolated) benzene,²³ with the results that $U = 16.93$ eV, $V = 9.027$ eV, $X = 3.313$ eV, and $W = 0.462$ eV. Thus, the typical range of parameters is $U > V > X > W$. To obtain a more intuitive feeling for how these parameters might vary in quasi-one-dimensional conjugated polymers, we turn to a very simple model that permits us to incorporate the two most significant physical effects determining U , V , X , and W . If we assume naively that the interaction is just the Coulomb potential (possibly suppressed by a constant dielectric function), the *relative* sizes of the parameters will be determined solely by the localization length—call it $1/\kappa_0$ —of the Wannier functions, ϕ . In practice, in the solid-state materials, the Coulomb potential affecting π electrons on a single chain may be screened both by the effects of π -electron motion on neighboring chains and by σ electrons on the same chain; a screening length—call it ζ —can be introduced to model these effects.

A simple but consistent one-dimensional model incorporating these effects begins with the Kronig-Penny model for the potential arising from the ions:

$$-\left[\frac{\hbar^2}{2m} \right] \frac{d^2}{dx^2} \Psi_k(x) + V_{\text{KP}}(x) \Psi_k(x) = \epsilon_k \Psi_k(x), \quad (2.3a)$$

where

$$V_{\text{KP}}(x) = - \left[\frac{\hbar^2 \kappa_0}{m} \right] \sum_n \delta(x - na). \quad (2.3b)$$

The localized atomic orbitals (for a single δ function) are then

$$\chi_n = \sqrt{\kappa_0} e^{-\kappa_0|x - na|}. \quad (2.3c)$$

Since these atomic orbitals are not orthogonal, to solve this problem completely, one should calculate the true eigenfunctions $\Psi_k(x)$ and Wannier function $\phi(x)$ given by

$$\phi(x) = \frac{1}{\sqrt{N}} \sum_k \Psi_k(x).$$

However, in the tight-binding limit ($\kappa_0 a \gg 1$), the true Wannier functions closely resemble these atomic orbitals. Notice that if this tight-binding limit is not at least approximately valid, many additional effects—for example, second-neighbor hopping—must be added to the model Hamiltonian, and the entire framework must be reexamined. Thus, consistent with our other approximations, we assume tight binding and approximate the Wannier functions by atomic orbitals for purposes of determining the sizes of the Coulomb parameters analytically. We also have computed the true Wannier functions numerically. The atomic orbitals and true Wannier functions are compared in Fig. 2.

First we examine the hopping integral for this model. By solving for the allowed spectrum of the period KP model, assuming $\kappa_0 a \gg 1$, and equating the actual band-

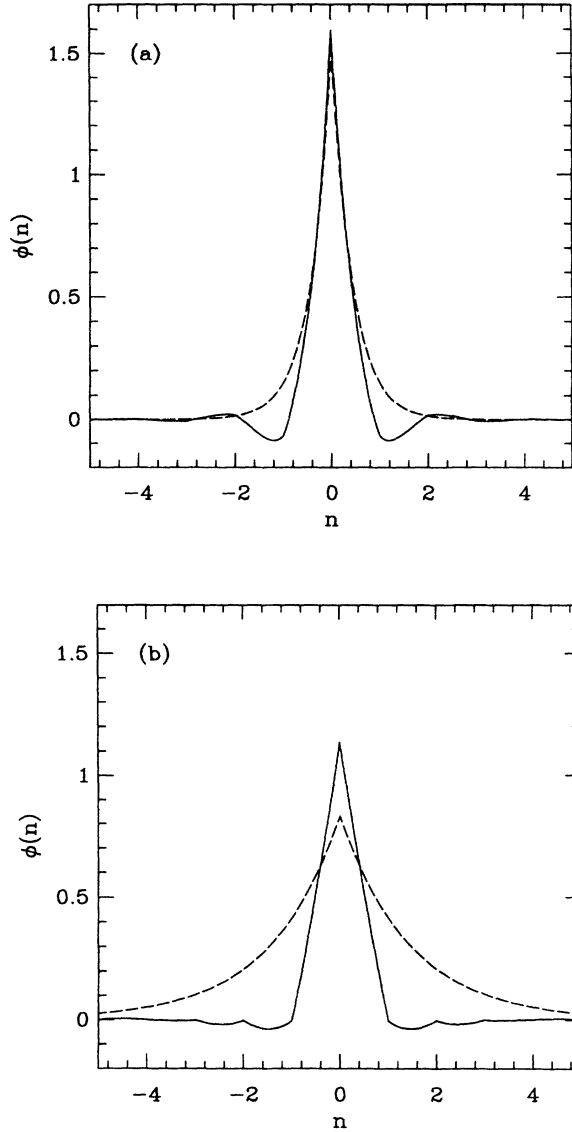


FIG. 2. Wannier function (solid) and atomic orbital (dotted) for the Kronig-Penny model with (a) $\exp(-\kappa_0 a) = 0.1$ and (b) $\exp(-\kappa_0 a) = 0.5$. For case (b), the tight-binding approximation is not good.

TABLE I. The numerical values of the nearest-neighbor hopping integral t_0 , its derivative α with respect to the lattice spacing a , and the second to fifth neighbor hopping integrals t_n , $2 \leq n \leq 5$, in units of $(\hbar^2/2ma^2)$. The values in parentheses are calculated from the approximate bandwidth [Eq. (2.4)].

	$\kappa_0 a = \ln 10$	$\kappa_0 a = \ln 2$
t_0	1.26(1.06)	0.35(0.48)
αa	3.52(2.44)	0.19(0.33)
t_2	-0.15	0.21
t_3	0.03	0.07
t_4	-0.01	-0.02
t_5	0.00	-0.04

width with $4t_0$ (the band width of a one-dimensional tight-binding model with bare hopping t_0) we find

$$t_0 \simeq \frac{\hbar^2}{2ma^2} 2(\kappa_0 a)^2 e^{-\kappa_0 a} \quad (2.4a)$$

and

$$\alpha a \equiv \frac{d}{da} (-t_0) \simeq \frac{\hbar^2}{2ma^2} 2(\kappa_0 a)^3 e^{-\kappa_0 a}. \quad (2.4b)$$

More precisely, the hopping integrals $t_{l,l'}$ between sites l and l' are calculated from⁷

$$t_{l,l'} = -\frac{1}{N} \sum_k \varepsilon_k e^{ik(l-l')a}, \quad (2.4')$$

where ε_k are the eigenvalues from Eq. (2.3a). Consistent with the conventions of the literature, we denote the nearest-neighbor hopping ($l-l'=1$) by t_0 but the further-neighbor hopping ($l-l'=n, n \geq 2$) by t_n (t_1 is typically reserved for a symmetry-breaking nearest-neighbor term). The numerical values of t_0 , αa , and the further-neighbor hopping integrals t_n are listed in Table I.

To introduce variable-range screening consistently within our one-dimensional kinematics, we take $V_{e-e}(x) = (ga/2\xi)e^{-|x|/\xi}$. Notice that for the extreme-screening limit, $\xi \rightarrow 0$, this reduces to a δ function. Then, introducing $\beta \equiv 1/\kappa_0 \xi$, $\gamma^{-1} \equiv 2 + \beta$, $\delta^{-1} \equiv 4 - \beta^2$ and employing equations (2.2a)–(2.2d) and (2.3), we find

$$U/g = \kappa_0 a \beta \gamma^2 (4 + \beta), \quad (2.5a)$$

$$V/g = \kappa_0 a \beta \delta [16\delta e^{-a/\xi} - \beta(1 + 2\kappa_0 a + 8\delta)e^{-2\kappa_0 a}], \quad (2.5b)$$

$$X/g = \kappa_0 a \beta \delta e^{-\kappa_0 a} \left[8\gamma \left[1 + \frac{1}{\beta} \right] - \frac{3\beta}{2} e^{-a/\xi} \frac{8\gamma}{\beta} + e^{-2\kappa_0 a} \frac{\beta}{2} \right], \quad (2.5c)$$

$$W/g = \frac{\kappa_0 a \beta e^{-2\kappa_0 a}}{2} \left[\gamma + \frac{2\kappa_0 a}{\beta} + 2\gamma^2 e^{-a/\xi} + \frac{2\gamma^2 (e^{-a/\xi} - 1)}{\beta^2 \delta} \right]. \quad (2.5d)$$

The separate dependence on the screening (ξ) and overlap (κ_0) parameters is apparent.

From the form of (2.5) one can see that U , V , and all the longer-ranged *diagonal* terms will always contain

contributions dependent only on the range of the potential—here determined by ξ —and not suppressed by the overlap factor ($e^{-\kappa_0 a}$). This is clearly the origin of the familiar result that for narrow bands, for which

TABLE II. The values calculated from the true Wannier functions (and from the atomic orbitals) of the Coloumb parameters for various ratios of the overlap (κ_0) and screening (ζ) parameters. In the table we have taken $\kappa_0 a = \ln 10$. An important qualitative difference between the two cases is the possibility that, for strong screening, the X term calculated using the Wannier function can be negative.

	$\kappa_0 \zeta = 4$	$\kappa_0 \zeta = 2$	$\kappa_0 \zeta = 1$	$\kappa_0 \zeta = \frac{1}{2}$	$\kappa_0 \zeta = \frac{1}{30}(0)$
V/U	0.6600(0.6855)	0.4453(0.5367)	0.2185(0.2704)	0.0738(0.1081)	0.0149(0.0561)
X/U	0.0079(0.2845)	0.0095(0.2565)	0.0058(0.2143)	-0.0046(0.1810)	-0.0223(0.1495)
W/U	0.0010(0.0488)	0.0021(0.0446)	0.0038(0.0392)	0.0057(0.0340)	0.0074(0.0280)

$t_0 \sim e^{-\kappa_0 a}$ is very small, the diagonal Coulomb terms are dominant. Note, however, even if the band is not narrow, if the potential is not strongly screened, one still expects the diagonal terms to be more important numerically than the off-diagonal terms. In Table II we present values of U , V , X , and W determined from (2.5) for a range of ζ and κ_0 , as well as the values calculated numerically using the true Wannier functions. In general, we see $U > V > X > W$. In the extreme screening limit ($\zeta \rightarrow 0$), using atomic wave functions, we find from (2.5) that $U = g\kappa_0 a$,

$$V = g\kappa_0 a (1 + 2a\kappa_0) e^{-2\kappa_0 a} = 2W,$$

and $X = \frac{3}{2}g\kappa_0 a e^{-\kappa_0 a}$; thus here one has $U > X > V = 2W$. Use of the true Wannier functions gives even smaller values for W and X , as well as a negative value for X in the extreme screening limit.

When the off-diagonal terms are not *a priori* negligible, the central issue is the extent to which they produce results qualitatively different from those predicted in their absence. To answer this question correctly, it is clear that—whatever the relative values of V , X , and W —one *must* anticipate that $U > V, X, W$ and hence must adopt a method that gives correct results in this parameter regime. Since, as we shall see, U does not contribute to first-order weak-coupling perturbation theory, these first-order predictions are likely to be unreliable in the expected parameter regime and for consistency one is compelled to go at least to second order. Actually, since in many materials one expects $U \simeq 4t_0$, to be certain of the results one should use (numerically) exact many-body methods known to be reliable in the intermediate-coupling regime. Further, to gain insight into the results of these methods, strong-coupling perturbation expansions should be studied. In the ensuing sections, we discuss all these approaches.

III. LIMITING BEHAVIOR

A. Weak-coupling perturbation theory

1. Second-order perturbation theory

To compare with previous results,¹⁶ we first study the model in the weak-coupling perturbation theory valid for small e - e couplings. Differentiating the energy, $E(\delta)$, for a uniform dimerization, $\delta_l = (-1)^l \delta$, one can obtain an implicit equation for the dimerization δ_0 which yields the minimum energy, $\partial E / \partial \delta|_{\delta_0} = 0$. Expanding about the minimum-energy value of the dimerization for $U = V = X = W = 0, \delta_{00}$, we obtain in Appendix A an expression for the linear shift in δ_0 to second order in the couplings:

$$\delta_0 / \delta_{00} - 1 = C_{U_i} U_i + C_{U_i, U_j} U_i U_j + O(U_i U_j U_k), \quad (3.1)$$

where $[U_i] = [U, V, X, W] / 2t_0$. We have evaluated the coefficients numerically for a range of parameters and system sizes, and representative values are listed in Table III.

In first order in the U_i one obtains (see Appendix A) the analytic result:

$$\delta_0^{(1)} / \delta_{00} - 1 = c_v \left[\left[\frac{4\pi\lambda}{1-d} \right] X - 6W + V \right], \quad (3.2)$$

where c_v is a positive coefficient related to elliptic functions,

$$d = (\pi\lambda / 2N) \left\langle \sum_l B_{l, l+1} \right\rangle,$$

and $\pi\lambda = 2\alpha^2 / t_0 K$. This agrees with the previous perturbation-theory results,^{16,28} except that these earlier

TABLE III. Values for various λ of the coefficients in Eq. (3.1), the expansion for weak correlations of the dimerization amplitude. Here $[u, v, w, x] = [U, V, W, X] / 2t_0$ and $\delta \rightarrow \alpha\delta_{00} / t_0$, and we have collected terms in a manner convenient for the weak-coupling analysis.

λ	N	δ	$+(v - 6w)$	$+x$	$+u^2$	$-uv$	$-v^2$	$-(v - 6w)^2$	$+xv$	$+xw$	$+x^2$
0.150	98	0.0525	3.708	9.970	1.297	2.079	3.646	-2.694	41.53	248.86	88.73
	100	0.0531	3.375	9.071	0.993	1.722	3.240	-3.163	41.54	249.34	85.70
0.204	98	0.1303	1.456	6.234	0.341	0.383	1.242	0.752	5.92	35.54	34.57
0.204	100	0.1303	1.456	6.234	0.305	0.366	1.220	0.757	5.92	35.58	34.57
0.250	74	0.2106	0.775	4.712	0.101	0.015	0.625	0.622	0.02	0.16	17.92
0.250	76	0.2106	0.775	4.712	0.127	0.085	0.637	0.625	0.04	0.17	17.99

studies ignored the X term entirely, assuming that it was negligible in a dimerized state.¹⁶ As our calculations show, this is true only for $\lambda \ll 1$. For normal polyacetylene parameters ($\lambda = 0.204$, $d \sim 2\lambda$) even in the extreme screening limit for which $V = 2W$, $\delta_0^{(1)}/\delta_{00} - 1$ is positive (and dimerization is enhanced) for

$$X > X_c = 0.24(6W - V) \sim W.$$

However, since for realistic parameters $U \gg (V, X, W)$, first-order perturbation theory is not a reliable guide even for weak Coulomb interactions. The most important term in second order, C_{UU} , is negative for large to intermediate λ . For weak effective e -ph couplings (and not-too-small rings), however, $C_{UU} > 0$, supporting the well-known observation that δ increases with weak interactions.^{2,8-15} V suppresses dimerization in second order since C_{VV} is negative, but the first order enhancement dominates. W suppresses and X enhances dimerization in second order.

In Fig. 3 the shift in the dimerization is shown for the values of the couplings obtained from the Kronig-Penny model. To summarize, if one consistently includes all terms through second order, U , V , and X enhance dimerization while W suppresses it. Overall Coulomb interactions enhance dimerization. This agrees with the numerical diagonalizations and strong-coupling arguments that follow, except as regards the behavior of W . Here, however, one must be careful to note that in both the numerical diagonalizations and strong-coupling arguments that the values of U (and occasionally V as well) are intermediate to large and hence outside the range of validity of perturbation theory. Since the perturbation-theory arguments assume that U , V , X , and W are all small and comparable, this disagreement is neither worrying nor surprising.

2. "g-ology"

Although not strictly a finite order, weak-coupling perturbation theory, the familiar studies known as "g-ology"^{29,30} amount to the summation of the (logarithmically) leading terms in all orders of (weak-coupling) perturbation theory. These g-ology studies²⁶ show that for weak e - e interactions, superconducting states—both singlet and triplet—can be favored for certain ranges of the parameters X , U , V , and W . These results are not in any obvious disagreement with our results, discussed in the following, that establish for *intermediate* to *strong* values of the normal "diagonal" Coulomb repulsions U and V , the ground state becomes a ferromagnetic phase. In particular, in connection with the possibility of triplet superconductivity, we will show below that if W can increase without limit, the ferromagnetic (FM) state will, for any fixed value of V , eventually become the ground state; we note also that this result is also confirmed by recent work

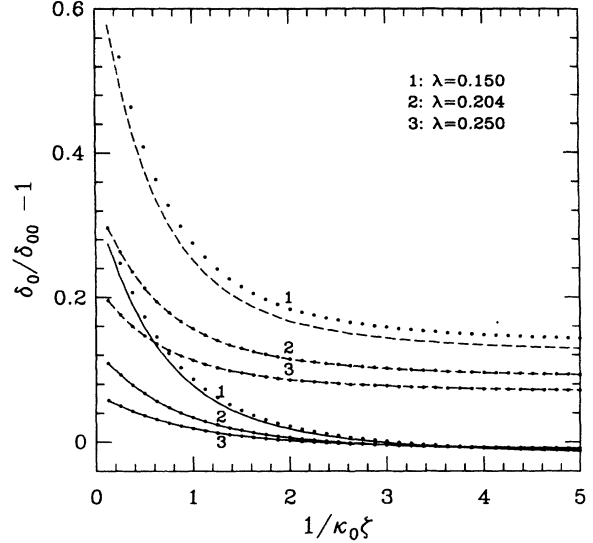


FIG. 3. $(\delta_0/\delta_{00} - 1)$, calculated from second-order weak-coupling perturbation theory using the coefficients at λ and N from Table III, for the atomic wave functions (Jahn-Teller, dashed; nonJahn-Teller, dotted) and the true Wannier functions (Jahn-Teller, solid; nonJahn-Teller, dotted) of the Kronig-Penny model, vs $\kappa_0\xi$. V/U , X/U , and W/U for representative values of $\kappa_0\xi$ are given in Table II. For this figure we have taken $U/2t_0 = 0.1$.

of Hirsch,²¹ who generates a ferromagnetic interaction by focusing on values of W which are effectively in the strong-coupling regime.

B. Strong-coupling perturbation theory

To complement our weak-coupling analysis and to provide intuitive interpretations for the results of our exact diagonalizations, we next analyze the Hamiltonian (2.1) in the strong-coupling limit. More precisely, we consider two related but distinct strong-coupling regimes: (1) the conventional $U \rightarrow \infty$ limit; and (2) the $t_0 = \alpha = X = 0$ limit, in which no single-particle hopping occurs. For the purpose of this analysis we find it convenient to rewrite H using spin (S_i) and "pseudospin" (σ_i) operators:

$$S_i^z = \frac{1}{2}(n_{i,\uparrow} - n_{i,\downarrow}), \quad S_i^+ = c_{i,\uparrow}^\dagger c_{i,\downarrow}, \quad \text{and} \quad S_i^- = c_{i,\downarrow}^\dagger c_{i,\uparrow};$$

$$\sigma_i^z = \frac{1}{2}(n_i - 1), \quad \sigma_i^+ = c_{i,\uparrow}^\dagger c_{i,\downarrow}^\dagger, \quad \text{and} \quad \sigma_i^- = c_{i,\downarrow} c_{i,\uparrow}.$$

The singly occupied sites have their normal spin notation, $|\uparrow\rangle$ and $|\downarrow\rangle$. The zero- and doubly occupied sites are denoted respectively by $|-\rangle$ ($\sigma^z = -\frac{1}{2}$) and by $|+\rangle$ ($\sigma^z = +\frac{1}{2}$). Note that $S_i^+ \sigma_i^- = \sigma_i^+ S_i^- = 0$ —i.e., a given site cannot have both nonzero spin and nonzero pseudospin—which follows trivially from their definitions. In these variables the Hamiltonian becomes

$$H = - \sum_i [t_0 - 2X(1 + \sigma_i^z + \sigma_{i+1}^z) - \alpha \delta_i] B_{i,i+1} + \frac{1}{2} K \sum_i \delta_i^2 - 4W \sum_i \mathbf{S}_i \cdot \mathbf{S}_{i+1} + 2U \sum_i \sigma_i^z \sigma_i^z$$

$$+ 4W \sum_i \left[\frac{1}{2} (\sigma_i^+ \sigma_{i+1}^- + \sigma_i^- \sigma_{i+1}^+) + \left(\frac{V}{W} - 1 \right) \sum_i \sigma_i^z \sigma_{i+1}^z \right] + (U + 4V) \sum_i \sigma_i^z + (V + W) N. \quad (3.3)$$

The first term, which involves single-particle hopping, is the only term which connects spin and pseudospin states (on adjacent sites). The third term is an isotropic ferromagnetic exchange of strength $4W$, involving only spin operators. The rest of the terms involve only pseudospin operators. The fourth term is a measure of double occupancy and the fifth term is a pair hopping and a repulsive or attractive V -like term, depending on the relative magnitudes of V and W . The last two terms just shift the zero of energy. Note (1) that when $\sigma_i^z + \sigma_{i+1}^z = 0$, as it is in the FM and extreme charge-density-wave (CDW) phases discussed below, the only effect of X is to renormalize t_0 to $t_X \equiv t_0 - 2X$; and (2) that the fifth term is the Hamiltonian of the one-dimensional XXZ spin chain³¹ with z -component coupling $\gamma = V/W - 1$.

1. The $U \rightarrow \infty$ limit and spin-Peierls theory

In the limit that $U \rightarrow \infty$, double occupancy of any site is energetically not allowed and, for the half-filled band, the ground state is described entirely in terms of spin states (zero pseudospin). Acting on these spin states, the Hamiltonian (3.3) will either produce new spin states (call these terms H_0) or they will produce (the suppressed) double occupancy and hence will couple spin states only indirectly through excitations to virtual pseudospin states (call these terms H'). In second-order perturbation theory, one has formally

$$H_{\text{eff}} = H_0 - \frac{H'^2}{\Delta}, \quad (3.4)$$

where Δ is the energy of the virtual states above the spin manifold. Clearly, only the effective single-particle hopping term contributes to H' , for which $\Delta \sim U - V$,³² and (3.4) yields

$$H_{\text{eff}} = \frac{1}{2}K \sum_l \delta_l^2 + (V + W)N - 4W \sum_l \mathbf{S}_l \cdot \mathbf{S}_{l+1} - \frac{\left[\sum_l t_{l,X} B_{l,l+1} \right]^2}{U - V}, \quad (3.5)$$

where $t_{l,X} = t_X - \alpha \delta_l$. Expanding the last term keeping only those terms which connect spin states, we thus see that, in this limit, the Hamiltonian (3.3) reduces to the effective spin-Peierls Hamiltonian^{11,19}

$$H_{\text{eff}} = \frac{1}{2}K \sum_l \delta_l^2 + NV = \sum_l \left[\frac{t_{l,X}^2}{U - V} - W \right] (4\mathbf{S}_l \cdot \mathbf{S}_{l+1} - 1). \quad (3.6)$$

The main effect of W , then, is to suppress antiferromagnetism. Further, to lowest order in δ_l , the spin coupling is proportional to

$$t_{l,X}^2 - W(U - V) \simeq [t_X^2 - W(U - V)] - 2\alpha t_X \delta_l + O(\delta_l^2) \equiv t'^2 - 2\alpha' t' \delta_l + O(\delta_l^2), \quad (3.7)$$

where

$$t' \equiv [t_X^2 - W(U - V)]^{1/2} \quad \text{and} \quad \alpha' = \alpha \frac{t_X}{t'}.$$

For given t_0 and X , since the effective t' decreases with W , the effective e -ph coupling $\pi\lambda' \equiv 2\alpha'^2/kt'$ increases with W due both to the increase in α' and the decrease in t' . This leads to the initially surprising conclusion that, for large U , the dimerization should initially increase with W , the bond-bond repulsion. This result is confirmed by the exact calculations of Sec. IV.

In the limit described by (3.6), when W reaches a critical value $W_c \simeq t_X^2/(U - V)$, the spin coupling becomes ferromagnetic. The spins will tend to align, forming a ferromagnetic (FM) phase with $4\mathbf{S}_l \cdot \mathbf{S}_{l+1} \simeq 2$, so that the effective Hamiltonian reduces to

$$H_{\text{eff}} \simeq \frac{1}{2}K \sum_l \delta_l^2 + NV. \quad (3.8)$$

The minimum-energy configuration thus has $\delta_l = 0$ and $E = NV$. Hence, in the $U \rightarrow \infty$ limit, our strong-coupling argument shows that for large W the ground state of (2.1) for the half-filled band is an undimerized FM phase with energy $E = NV$. Again, these results are confirmed by the exact diagonalization of Sec. IV B.

2. The zero-hopping limit and pseudospin theory

We can explore a different region of the "phase" diagram of (2.1) by ignoring all (linear) hopping terms—thus setting $t_0 = \alpha = X = 0$ —and considering only U , V , and W . As we shall see, this limit also provides useful insight into our exact diagonalization results.

To begin we consider the additional simplification $W = 0$. Then, since U and V are diagonal in the site representation, it is straightforward to analyze the possible ground states. For $U > 2V$, the phase with each site singly occupied is the ground state. For latter convenience, we call this a spin-density wave (SDW), although strictly speaking the many degenerate spin configurations lead to no fixed spin periodicity; further, since in the absence of W and t_0 all spin alignments are degenerate, this phase is *not* the FM phase seen in the large W limit. In fact, this is just the phase that in the presence of nonzero t_0 and α , would be the normal BOW. For $U < 2V$, the phase with each alternate site doubly occupied is the ground state. This is clearly a CDW. Since $W > 0$,³³ interfaces between regions of spins and pseudospins will cost energy, so the ground state will still have only one phase: either all spins (SDW) or all pseudospins (CDW).

As shown in the previous subsection, for nonzero W —but $t_0 = \alpha = X = 0$ —the pure spin phase is a FM phase with energy $E = NV$. In the pseudospin (CDW) phase, the effective Hamiltonian is

$$H_{\text{PS}} = N\left(\frac{1}{2}U + V + W\right) + 4W \sum_l \left[\sigma_l^x \sigma_{l+1}^x + \sigma_l^y \sigma_{l+1}^y + \left(\frac{V}{W} - 1\right) \sigma_l^z \sigma_{l+1}^z \right]. \quad (3.9)$$

As already noted, the term involving the σ operators in

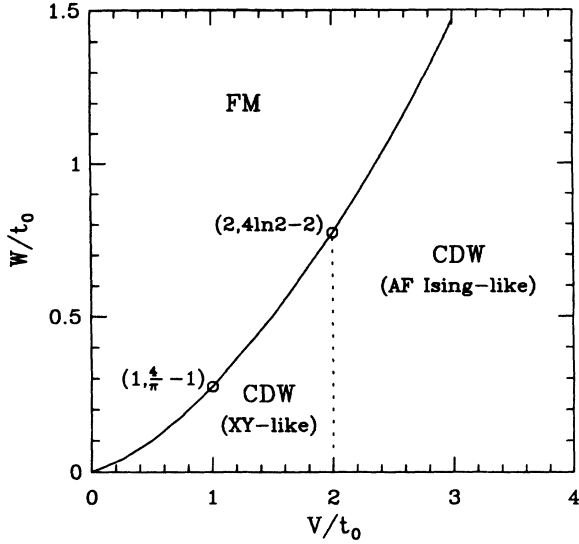


FIG. 4. The phase diagram of the Hamiltonian (2.1) in the zero-hopping limit $t, \alpha, X \rightarrow 0$.

(3.9) is the Hamiltonian of the one-dimensional XXZ spin chain.³¹ Thus the ground-state energy in the pseudospin phase is

$$E_{\text{PS}} = N \left[\frac{1}{2}U + V + W - Wf \left[\frac{V}{W} - 1 \right] \right], \quad (3.10)$$

where $-f(\gamma)$ is the per site ground-state energy of the XXZ spin chain, with Hamiltonian

$$H_{XXZ} \equiv 4 \sum_l (\sigma_l^x \sigma_{l+1}^x + \sigma_l^y \sigma_{l+1}^y + \gamma \sigma_l^z \sigma_{l+1}^z). \quad (3.11)$$

The FM-CDW phase boundary is therefore determined by

$$V_1 = \frac{1}{2}U + V + W - Wf \left[\frac{V}{W} - 1 \right]. \quad (3.12)$$

$$Z = \text{Tr} T_\tau \int \mathcal{D}\delta_l(\tau) \exp \left[- \int_0^\beta d\tau \left[\sum_l \left[\frac{1}{2}K \delta_l^2(\tau) + \alpha \delta_l(\tau) B_{l,l+1} \right] + H_e \right] \right].$$

The Gaussian integrals over $\delta_l(\tau)$ can be performed, yielding

$$Z = \text{Tr} \exp \left[-\beta \left[H_e - \frac{\alpha^2}{2K} \sum_l B_{l,l+1}^2 \right] \right].$$

Thus in this antiadiabatic limit we see that the e -ph coupling produces an *effective bond-bond attraction*:

$$W_{\text{eff}} = W - \frac{\alpha^2}{2K}.$$

From the known results for the XXZ chain,³¹ we have $f(-1)=1$, $f(0)=4/\pi$, and $f(\gamma) \rightarrow |\gamma|$ for $\gamma \rightarrow \pm\infty$. Thus in the $U/2W$ versus V/W plane, the phase diagram is as sketched in Fig. 4. In particular, for $W \rightarrow 0$ we find

$$V \simeq \frac{1}{2}U + 2W \quad (3.13)$$

as the boundary between the CDW (large V) and FM (small V) phases. Although nonzero hopping shifts the boundary, Eq. (3.13) gives good agreement with the exact diagonalization results of Sec. IV in the region $W, V, U \gg t_0$.

Finally, we note that this strong-coupling analysis also shows that within the CDW phase there is a second-order transition at $V=2W$ from an XY -like to an antiferromagnetic Ising-like CDW. Since the parameter range involved is unlikely to be relevant for real materials, we have not looked for this effect in our exact diagonalizations.

C. Antiadiabatic limit

Up to now we have ignored the quantum nature of the lattice. We turn now to briefly discuss the effects of quantum fluctuations of the lattice on the dimerization by considering the unphysical limit of the mass of the (CH) unit going to zero—the antiadiabatic limit. Fradkin and Hirsch³⁴ show that for spin- $\frac{1}{2}$ electrons at half-filling the properties of the system near the dimerization transition at small but finite mass are controlled by the behavior at $M=0$. For $M=0$ the phonons can be integrated out in a manner that allows simple interpretation of the resulting effective e - e interaction. The statistical mechanics of the Hamiltonian can be constructed from the partition function

$$Z = \text{Tr} \exp(-\beta H).$$

Reformulating Z as a path integral and setting the (CH) unit mass to zero, we find

However, for $W_{\text{eff}} < 0$ this term does not cause a *static BOW* distortion, though the correlation functions

$$\mathcal{B}_{\text{BOW}}(q) = \left\langle \left[\sum_l \cos(ql) B_{l,l+1} \right]^2 \right\rangle$$

are not zero. For $W_{\text{eff}} > 0$ the FM phase discussed above is found. Thus, even this extreme limit, the above strong-coupling considerations are qualitatively correct. We do not expect quantum phonons to significantly alter the phase diagram for realistic masses, and we do not

consider them further. For a more detailed analysis of the effects of finite phonon frequencies in the “g-ology” approach, see Ref. 26.

IV. EXACT DIAGONALIZATIONS

A. Analytic results for the ground state of the dimer

As a prelude to our (numerical) exact diagonalizations, we present the analytic results for the half-filled “dimer”—that is, two electrons on two sites—described by the Hamiltonian in (2.1). Although its limited size does lead to a few artifacts, the dimer provides surprisingly accurate insight into many aspects of the behavior of the larger system, and thus we find it instructive to present the analysis in detail.

For comparison with the numerical results, we use periodic boundary conditions, so that $c_3^\dagger = c_1^\dagger$ and similarly for all other operators. Incorporating these conditions and restricting the sums in (2.1) to $l=1,2$ yields the explicit Hamiltonian

$$H_d = -2[t_0 - X(n_1 + n_2)]B_{1,2} + U(n_{1\uparrow}n_{1\downarrow} + n_{2\uparrow}n_{2\downarrow}) + 2Vn_1n_2 + 2W(B_{1,2})^2, \quad (4.1)$$

where the factors of 2 arise from the periodic boundary conditions. Since there is no possibility of bond alternation with only one bond, no explicit e -ph coupling appears, and the hopping term is simply taken as t_0 . Further, in the half-filled dimer one has $n_1 + n_2 \equiv 2$; thus just as in the case of the $U \rightarrow \infty$ limit discussed in Sec. III B, the X term simply renormalizes the hopping to $t \equiv t_0 - 2X$.

Simple counting shows that there are six possible states for two electrons on two sites. As basis states we choose

$$\begin{aligned} |1,1\rangle &\equiv c_{2\uparrow}^\dagger c_{1\uparrow}^\dagger |0\rangle, \\ |1,0\rangle &\equiv \frac{1}{\sqrt{2}}(c_{2\downarrow}^\dagger c_{1\uparrow}^\dagger + c_{2\uparrow}^\dagger c_{1\downarrow}^\dagger) |0\rangle, \\ |1,-1\rangle &\equiv c_{2\downarrow}^\dagger c_{1\downarrow}^\dagger |0\rangle, \\ |0,0\rangle &\equiv \frac{1}{\sqrt{2}}(c_{2\downarrow}^\dagger c_{1\uparrow}^\dagger - c_{2\uparrow}^\dagger c_{1\downarrow}^\dagger) |0\rangle, \\ |S\rangle &\equiv \frac{1}{\sqrt{2}}(c_{1\uparrow}^\dagger c_{1\downarrow}^\dagger + c_{2\uparrow}^\dagger c_{2\downarrow}^\dagger) |0\rangle, \\ |A\rangle &\equiv \frac{1}{\sqrt{2}}(c_{1\uparrow}^\dagger c_{1\downarrow}^\dagger - c_{2\uparrow}^\dagger c_{2\downarrow}^\dagger) |0\rangle. \end{aligned}$$

As the notation suggests, the first three states are, respectively, the $S_Z = +1, 0$, and -1 components of the spin triplet state and, by the spin symmetry of H , must all have the same energy. The state $|0,0\rangle$ is a spin singlet made entirely from singly-occupied states, while $|S\rangle$ and $|A\rangle$ are, respectively, spin singlets made from symmetric and antisymmetric combinations of the two states involving double occupancies. Trivial algebra leads to the following results: (1) the triplet states are threefold degenerate eigenstates of H_d , with eigenvalue $E_T = 2V$; (2) the state $|A\rangle$ is also an eigenstate, with eigenvalue U ; and (3) the states $|0,0\rangle$ and $|S\rangle$ are coupled, leading to a 2×2

matrix with eigenvalues

$$E_{\pm} = 8W + \frac{1}{2}U + V + \frac{1}{2}\Delta,$$

where

$$\Delta = [(U - 2V)^2 + (8t_0 - 16X)^2]^{1/2}.$$

The ground state “phase diagram” for the dimer follows immediately by comparing these eigenenergies. For $U \equiv U = 4t$ (intermediate coupling), this diagram as a function of W/t and V/t is shown in Fig. 5. The three different regions of the diagram are labeled by the nature of the ground state and the boundaries are indicated by the letters A through D .

For small values of W , in the region below the curves AB and BD , the state E_- is always the ground state. This state, which in the absence of e - e interactions is just the $k=0$ band state, corresponds to the “dimerized-BOW” phase and indeed, in the larger systems shows nonzero values of the dimerization parameter $\delta_i = (-1)^i \delta_0$. In the region bounded by AB and BC , the triplet state is the ground state; as our prior strong-coupling arguments suggest and our later exact calculations confirm, this corresponds to the ferromagnetic (FM) phase found in larger systems. Finally, in the region bounded by BC and BD , the ground state is the state $|A\rangle$, with energy U ; this corresponds to the CDW phase in larger systems.

The boundaries between the phases can be determined analytically. One finds that the BOW-FM boundary—line AB —is given by

$$W_{AB}(V) = \frac{1}{16} \{ (2V - U) + [(U - 2V)^2 + 64t^2]^{1/2} \}, \quad (4.2)$$

where $2V < U$, so that the value of W for which “dimerization” disappears for $V=0$ (point A) is, for the parameters in Fig. 5, $W_{AB}(0) = 0.31t$, while the “triple point” (B)

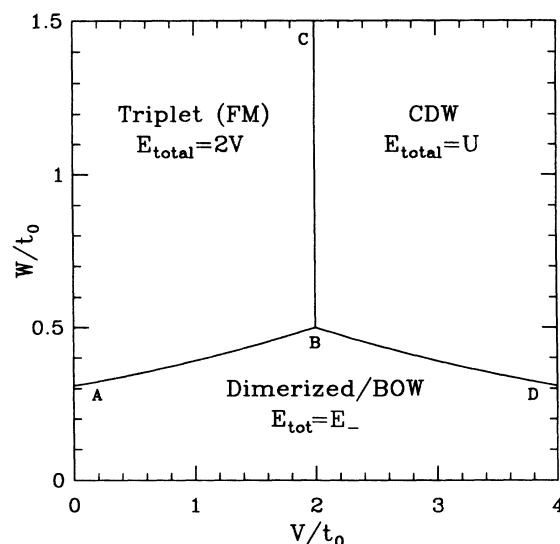


FIG. 5. The phase diagram as a function of V/t and W/t for the half-filled dimer for intermediate coupling $U = 4t = 4t_0 - 8X$.

occurs at $W=t/2$, $V=2t$, for $U=4t$.

The FM-CDW boundary is simply given by $2V=U$, independent of W . Our strong-coupling arguments suggest, and our numerical results confirm, that this is an artifact of the dimer and that in fact the boundary is at $2V \approx U + 4W$ in large systems.

Finally, the CDW-BOW boundary—line BD —is given by

$$W_{BD}(V) = \frac{1}{16} \{ (U - 2V) + [(2V - U)^2 + 64t^2]^{1/2} \}, \quad (4.3)$$

where $2V > U$. Hence, for the dimer, the “BOW” phase persists even as $V \rightarrow \infty$, with the critical value of W that destroys “dimerization” behaving as $W_c \sim 2t^2/(2V - U)$ for $V \rightarrow \infty$. As we shall see, this persistence of dimerization to large V is also an artifact of the dimer. For larger systems, the CDW state becomes the ground state (for $W=0$) near the (naive) estimate $2V=U$. Despite these artifacts, however, the dimer guides our intuition in a qualitatively accurate way and, combined with the strong-coupling arguments, allows us to interpret the exact-diagonalization results in an appealing and unambiguous manner.

B. Numerical studies of finite-size rings

To study the effects of off-diagonal e - e interactions in a definitive way in the region of intermediate coupling anticipated to apply to many novel materials, we have calculated numerically the “exact” ground state of finite rings described by the Hamiltonian (2.1) using a version of the Lanczos method.³⁵ The details of the approach are given in Appendix B. To demonstrate the convergence of our results as a function of system size, we investigate 4, 6, 8, and 10 site rings.

As in the previous sections, we focus on the phase dia-

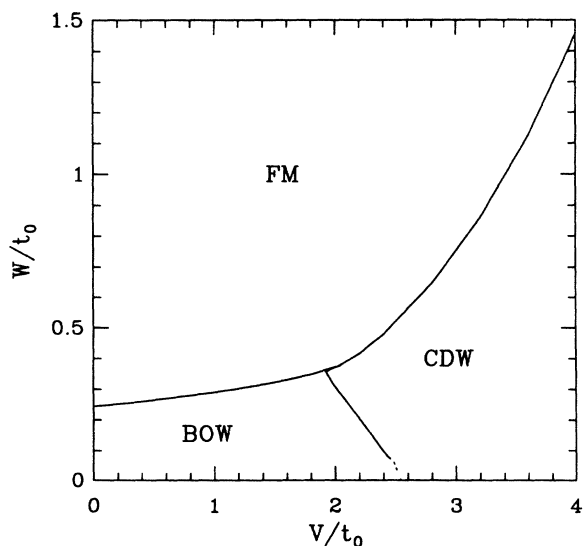


FIG. 6. The phase diagram as a function of V/t_0 and W/t_0 for intermediate coupling $U=4t=10$ eV, and $X=0$. Phase boundaries are plotted for an 8-site ring. The ground-state wave function changes discontinuously across solid lines, smoothly across the dotted line.

gram as a function of W and V at fixed U . Since weak coupling and strong coupling have been analyzed perturbatively above, we examine here values of U in the intermediate-coupling range; the $U=4t_0$ results shown in Fig. 6 are typical. Based on our earlier strong-coupling and dimer results, we anticipate that the primary effect of X (for these intermediate values of U) on the ground state and dimerization will be a renormalization of t_0 to $t \equiv t_0 - 2X$; we present data confirming this after discussing our other results. For comparison and definiteness, we use the conventional SSH-polyacetylene parameters $\alpha=4.1$ eV/Å, $K=21$ eV/Å², and $t_0=2.5$ eV. Hence $\lambda \equiv 2\alpha^2/\pi K t_0 = 0.204$.

In Fig. 6 we show the phase diagram, determined numerically by the Lanczos procedure described in Appendix B, for an 8-site ring; comparison with results on 4-, 6-, and 10-site rings suggests this diagram reflects the infinite-ring behavior. In Figs. 7 and 8 we show the actual value of δ_0 , the optimal dimerization, versus W for 4, 6, 8, and 10 site rings when $U=4t_0$ and $V=0$ or $V=0.3U$, respectively. Several points are immediately apparent from these figures.

First, the dimerized-BOW persists for a substantial range of Coulomb repulsion, both diagonal and off diagonal. In particular, as shown in Fig. 7, even for $V=0$, W does not destroy dimerization until $W_c \approx 0.24t_0 = 0.6$ eV. This agrees very well with our strong-coupling estimate of $W_c/t_0 \approx t_0/(U-V)$, which for $U=4t_0$, $V=0$ gives $W_c/t_0 = 0.25t_0$. Further, as also suggested by our strong-coupling estimates, the dimerization actually *increases* monotonically with W , before dropping rapidly to zero in a “first-order phase transition” at W_c . Thus, although the basic intuition that W opposes a BOW and will eventually destroy dimerization is correct, earlier

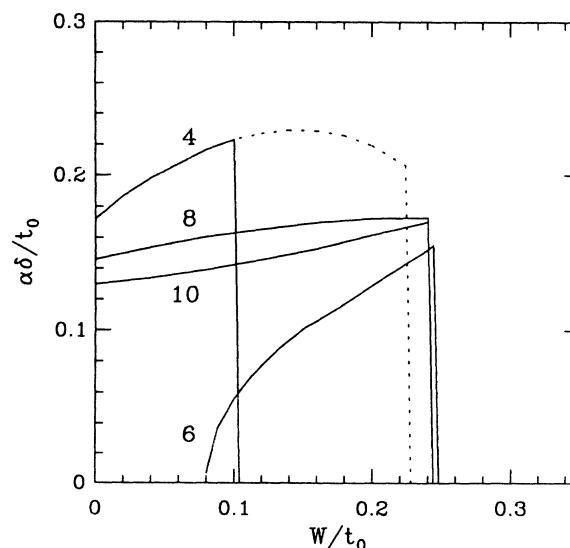


FIG. 7. Dimerization as a function of W/t_0 for $U=4t_0=10$ eV and $V=X=0$ for 4-, 6-, 8-, and 10-site rings. For the 4-site ring, the dotted line gives results for the lowest-energy dimerized state even though for this small ring the ground state is not dimerized for intermediate values $0.10 < W/t_0 < 0.225$ of W/t_0 .

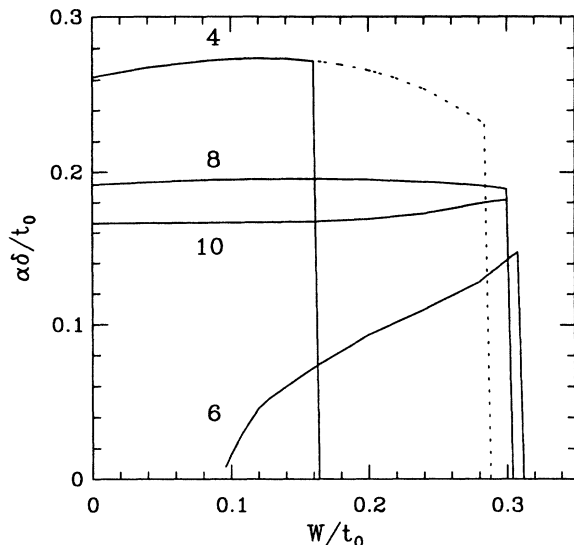


FIG. 8. Dimerization as a function of W/t_0 for $U=4t_0=10$ eV, $V=3$ eV, and $X=0$ for 4-, 6-, 8-, and 10-site rings. For the 4-site ring, the dotted line gives results for the lowest-energy dimerized state even though for this small ring the ground state is not dimerized for intermediate values $0.16 < W/t_0 < 0.29$ of W/t_0 .

conclusions—based on first-order perturbation-theory estimates¹⁶—that (for $V=0$) W should lead to a continuous and rapid decrease in dimerization are incorrect.

Second, for $0 < V < U/2$, the dimerized phase persists until still larger values of W , and again W increases dimerization (slightly) until the BOW-FM boundary is reached. This is indicated quantitatively in Fig. 8, in which the value of δ_0 versus W is plotted for $U=4t_0=10$ eV and $V=1.2t_0=3$ eV, again for 4, 6, 8, and 10 site

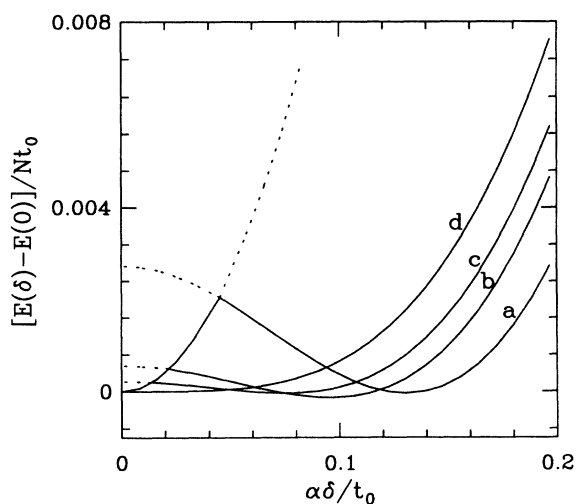


FIG. 9. The energy difference $E(\delta) - E(0)$ at the phase boundary in Fig. 6 between the BOW and CDW phases. The values of (V, W) are (a) (5.892 eV, 0.3 eV); (b) (6.084 eV, 0.2 eV); (c) (6.135 eV, 0.18 eV); and (d) (6.210 eV, 0.15 eV). As δ is decreased, these solid “BOW” curves become dotted as soon as the “CDW” solution becomes energetically favorable.

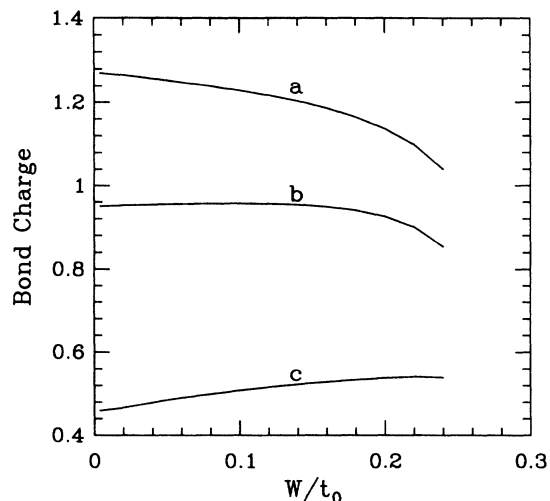


FIG. 10. Bond-charge measurements on the 8-site ring as a function of W/t_0 for $U=10$ eV and $V=0$: (a) bond-bond correlation (multiplied by $\frac{1}{2}$), (b) average bond charge, and (c) alternating bond charge, which is proportional to the dimerization.

rings. Note the increase in W_c ; consistent with Fig. 6, here we find $W_c(V=3) \approx 0.32t_0 = 0.8$ eV. Here our strong-coupling estimate that $W_c/t_0 \approx t_0/(U-V)$ gives $W_c \approx 0.36t_0 = 0.9$ eV. Further, the increase in dimerization versus W predicted by the strong-coupling arguments is still present, albeit in weaker form than for $V=0$. Note that this $V=3$ eV example is expected to show greater deviation than the $V=0$ case from the strong-coupling estimates, since it is nearer the $V \sim U/2$ boundary between the BOW and CDW phases where the

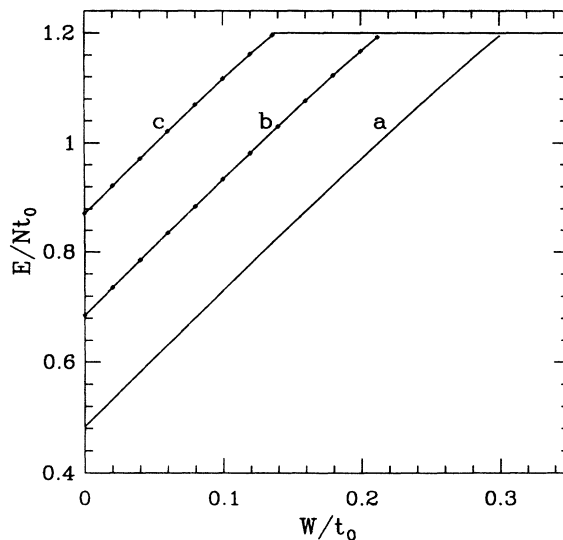


FIG. 11. Energy per site on the 8-site ring as a function of W/t_0 for $U=10$ eV and $V=3$ eV. For large W/t_0 , the ground-state energy for the FM is $E/N = V$, independent of W . For small W/t_0 , the curves are for (t, X) equal to (a) (2.5 eV, 0); (b) (2.5 eV, 0.25 eV) and (2.0 eV, 0); and (c) (2.5 eV, 0.5 eV) and (1.5 eV, 0). For parameter sets (b) and (c) the two different curves are indistinguishable on this scale.

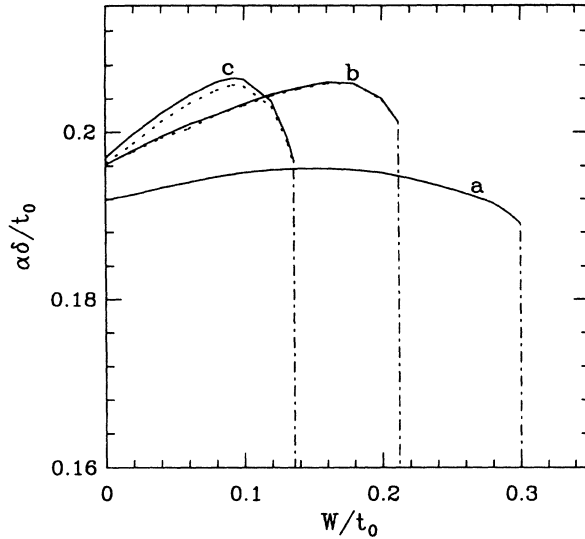


FIG. 12. Dimerization as a function of W/t_0 for the parameters of Fig. 11. In (b) and (c) the dotted lines are for $X=0$.

strong-coupling analysis of dimerization breaks down.

Third, both Figs. 7 and 8 show that the distinction between “Jahn-Teller” (here, $4N$) and “non-Jahn-Teller” ($4N+2$) system persists even away from the band-theory limit. However, they also suggest that systems with $N \geq 8$ are near the converged large- N behavior. Incidentally, the dotted regions of the 4-site ring results in Figs. 7 and 8 reflect the dimerization observed in the BOW phase. However, the actual ground state of the 4-site system at values of W in these dotted regions is a different, small-ring phase, which does not appear in the larger rings. Thus the solid line for the 4-site system, which shows the dimerization going to zero at relatively small values of W , although strictly correct, is essentially an artifact of the small-system size. The dotted line, which explicitly ignores this small-ring phase and plots the dimerization assuming the BOW state remains the ground state until the transition to the ferromagnetic phase, shows more clearly the true finite-size effects on W_c and on δ_0 vs W .

Fourth, the phase boundaries in Fig. 6 in general reflect a “first-order transition” in the dimerization order parameter, δ_0 : that is, there is a sudden qualitative change in the nature of the ground state, and δ_0 drops discontinuously from a finite value to zero. However, for the short segment of the BOW-CDW boundary near $W=0$ —the range is roughly $0 < W < 0.1$ eV—the transition becomes second order. This is shown in Fig. 9, which plots $E(\delta) - E(0)$ for points on the BOW-CDW boundary; for $W < 0.1$ eV, the transition becomes second order. Except for this short segment, the dimerized phase has nonzero dimerization on its boundary.

Increasing W , of course, must suppress bond-bond correlations. In Fig. 10, the bond-bond correlation, average bond charge, and alternating bond-charge are plotted as a function of W for intermediate coupling, $U=4t_0$ and $V=0$, on the 8-site ring. As we would expect, the bond-bond correlation $\langle B^2 \rangle = (1/N) \sum_l B_{l,l+1}^2$, which couples

directly to W in the Hamiltonian, is suppressed monotonically as W is turned on. Counter to naive intuition, however, the *average* bond charge, $\langle B \rangle = (1/N) \sum_l B_{l,l+1}$, does *not* fall off as dramatically as the correlation and indeed, for small W , the bond charge stays remarkably flat. Meanwhile, the *alternating* bond charge, which is related to the dimerization by

$$\langle B' \rangle = (1/N) \sum_l (-1)^l B_{l,l+1} = K\delta/\alpha,$$

increases with W , as we have seen earlier. In sum, while W must suppress bond-bond correlations, the effects on average and alternating bond charge may be quite different. In particular, we predict and observe that the dominant effect of W is to increase the effective e -ph coupling and so enhance the dimerization.

The effect of X on these results as indicated in Figs. 11 and 12. In Fig. 11, the ground-state energy at fixed V ($=3$ eV) is plotted versus W for three values of the effective hopping, t ; they are $t=2.5$ eV, $t=2.0$ eV, and $t=1.5$ eV. As expected from our strong-coupling analysis, the BOW-FM boundary moves to *lower* values of W as the effective hopping is decreased. In Fig. 11, the curve labeled (a) is for $t_0=2.5$ eV, $X=0$. That labeled (b) is actually two curves, one for $t_0=2.0$ eV, $X=0$ and one for $t_0=2.5$ eV, $X=0.25$ eV. They are indistinguishable on this scale. Similarly, the curve labeled (c) is again two curves: $t_0=1.5$ eV, $X=0$ and $t_0=2.5$ eV, $X=0.5$ eV. Clearly, for these values of $U(=4t_0)$ and $V(=1.2t_0)$, BOW-FM boundary behaves as suggested by the case of the dimer, depending only on $t \equiv t_0 - 2X$.

In Fig. 12 we show the effect of X on the dimerization versus W plot. The parameters and the labeling of the curves are the same as in Fig. 11. Again, the values of both W_c and δ are virtually indistinguishable. In case (c), however, one can see a slight enhancement ($\sim 0.3\%$) of dimerization with X ($t_0=2.5$ eV, $X=0.5$ eV) beyond what one would expect from simply renormalizing the band width ($t_0=1.5$ eV, $X=0$). Nevertheless, the overriding effect of X in intermediate to strong coupling is indeed to renormalize t_0 to $t = t_0 - 2X$. Thus as far as dimerization in the half-filled band is concerned, one can in effect use the $X=0$ results with t_0 determined by the actual band width to determine both δ and W_c ; if nonzero X is used, t_0 must be suitably increased to compensate, so that the actual band width, now given by $4t$, remains correct.

In summary, our exact diagonalizations confirm the results predicted from the weak-coupling, strong-coupling, and (analytic) dimer arguments. For intermediate strength e - e interactions, the BOW phase persists even in the presence of off-diagonal interactions. Within the dimerized phase, at fixed V dimerization actually increases (slightly) with W . Thus, at least for small values of W and for the range of e -ph couplings considered here, the extended Peierls-Hubbard models with *no* off-diagonal terms actually *underestimate* the enhancement of dimerization caused by Coulomb interactions! For large values of W —and fixed U and V —the off-diagonal Coulomb interactions generate a new ferromagnetic

phase. In view of our analysis in Sec. II on the relative sizes of the diagonal and off-diagonal terms, it remains unclear whether this range of parameters can be achieved in any real materials. Finally, the role of X , for the intermediate e - e interactions in the half-filled band, is primarily to renormalize t_0 to $t_0 - 2X$. We shall discuss further the implications of all these results for the modeling of real conducting polymers and other novel materials in the following section.

V. DISCUSSION AND CONCLUSIONS

Taken together with prior work, our combined weak- and strong-coupling perturbation-theory and exact-diagonalization results present a unified picture of the effect of short-ranged e - e interactions on dimerization in the half-filled band. Previous studies^{2,8-15} established that diagonal Coulomb repulsion terms (U, V) enhance dimerization substantially for intermediate values ($U \sim 4t_0, V < U/2$) and for small e -ph couplings ($\lambda \simeq 0.2$). Only for (unphysically) large value of λ do diagonal Coulomb interactions uniformly suppress dimerization.^{8,9} Our results establish that off-diagonal terms (W, X) of the same range and internally consistent magnitudes do *not* alter these results; even strong Coulomb interactions, provided the parameters are determined consistently, do not destroy dimerization.

Focusing first on W , we have shown that in half-filled band for intermediate U and V , the dimerization actually *increases* with the addition of (small) W . Further, the dimerization remains large until W reaches a critical value, W_c , at which point there occurs a (first order) phase transition between the dimerized BOW phase and the undimerized ferromagnetic phase that exists for large W . In real materials, the presence of such large values of W —for the given U and V —seems dubious but remains an open question. It is conceivable that the recently observed organic ferromagnetic materials may be modeled using parameters in this range. However, for $(\text{CH})_x$ and the other conjugated polymers, the experimentally observed dimerization requires, within the model Hamiltonian, $W < W_c$. Importantly, one still finds dimerization for strong, internally consistent Coulomb interactions; the assumption of weak e - e interactions is *not* required.^{10,16} This is fortunate, for in the case of $(\text{CH})_x$, such an assumption appears inconsistent with both observed spin density ratio³⁶ and optical absorption involving neutral and charged solitons.¹⁰

For intermediate strength U and V , the primary quantitative effect of including an “ X ” term in the case of the half-filled band is to renormalize the hopping term t_0 to $t \equiv t_0 - 2X$. This of course affects the values of the model parameters used to fit the properties of real materials, but for a given t , both δ within the dimerized phase and W_c remain virtually unchanged as t_0 and X are varied.

Regarding the values of the various model parameters, it is essential to recognize that they cannot be chosen or varied arbitrarily. All the e - e interaction parameters derive from the (possibly screened) Coulomb potential and, except for strong screening, one has $U > V > X > W$. In several real materials this ordering is confirmed by de-

tailed fits, and in particular one finds $U \gg W$. This inequality makes any first-order, weak-coupling perturbative treatment *a priori* suspect, since only V , X , and W enter in first order; the (generally much larger) U term enters only in second and higher orders. Indeed, our results suggest that to determine the true effects of e - e interactions for internally consistent values of the parameters, one must use methods that provide the correct solution to the many-body problem in the intermediate-coupling regime.

When one adds e - e interactions to a single-electron model describing real materials, it is essential to reevaluate the other interaction parameters to obtain a consistent fit to the full range of experimental observables. Previous studies of diagonal Coulomb forces^{2,8-15} have shown that the inclusion of intermediate strength U and V ($< U/2$) increases both the optical gap and the dimerization; hence, to fit the experimental data, one requires a *weaker* e -ph coupling (λ) when e - e interactions are included. In the case of off-diagonal terms in the half-filled band, the most prominent effect of this sort is the renormalization by the X term of the hopping, as already discussed. Clearly, to keep the full band width constant, one must increase t_0 if X is included.

In addition to these quantitative effects, the off-diagonal terms can have important qualitative consequences. The mixed bond-site term X breaks charge-conjugation–particle-hole symmetry; its inclusion in models of $(\text{CH})_x$ may thus help explain the puzzling “intensity anomaly” in polaron/bipolaron optical absorption³⁷ experiments and also the ratio of neutral ($S^0 - S^0$) to charged ($S^+ - S^-$) soliton pairs in the decay channels of electron-hole pairs in photoexcitation of trans- $(\text{CH})_x$.¹⁰ In both these cases, the X term may well be more important than the straightforward next-nearest-neighbor hopping term which we called t_2 above; within a tight-binding model, $t_2 \propto e^{-\kappa_0 a} t_0$. If X terms are included in H , the effective hopping acquires an effective band-filling dependence; this may be quite significant in applying Hubbard-like models to situations other than the half-filled band. For instance, if X is repulsive for electrons (near the bottom of a band) it will be attractive for holes (near the top of the band). As a consequence, the X term has recently been discussed as a possible source of electronically driven superconductivity.²⁰ One specific mechanism by which the “density-dependent hopping term” X can lead to superconductivity in a two-band, two-dimensional model is discussed in Ref. 38.

Finally, we turn to the general issue of the applicability of the standard Hubbard model. Here it is useful to place our work in the context of several recent articles that, in one way or another, have revisited the original analyses that justified the “zero differential overlap”^{1,23} approximation that neglects off-diagonal terms.^{4,7} First, we have shown that first-order perturbation theory¹⁶ is *not* a reliable basis on which to question the validity of the extended Hubbard model, since conclusions based on perturbation theory about the effects of off-diagonal terms on dimerization are not valid for realistic, self-consistent values of the Coulomb interaction parameters. Second, although our study focused explicitly on (an *exact* numer-

ical solution for) short-ranged Coulomb effects, involving only on-site and nearest-neighbor interactions, our results are consistent with two recent variational studies involving (approximate) solutions for the full (screened) Coulomb interaction. The first study used a Jastrow variational *ansatz*²⁴ to examine quantitatively the effect of e - e interactions on dimerization, and the second undertook a detailed qualitative analysis of the validity of the Hubbard model using only the assumption that the overlap integrals decay more rapidly with distance than does the interelectronic potential.²⁵ The results of both these studies are consistent with ours insofar as they can be related. For all except extremely short screening lengths and for weak (to intermediate) e -ph coupling, the variational results²⁴ show that dimerization is enhanced by Coulomb effects. Further, for this region of parameters, the variational results on the full Coulomb problem are consistent with early (Gutzwiller) variational calculations in the pure Hubbard model.³⁹ Similarly, for $\kappa_0 \hat{\zeta} \gg 1$ —so the overlap integrals fall off more rapidly than the e - e interactions²⁵—our results also establish that the extended Hubbard model correctly reflects the consequences of including *all* e - e interactions up to nearest neighbors. As discussed above and elsewhere,^{20–22,26} if the values of the X and W terms can be dialed at will, one can readily explain both (electronically driven) superconductivity and ferromagnetism. However, as we have argued, one cannot choose the values of these terms independent of the values of the normal U and V ; thus, barring some unusual structure in the Wannier functions, it seems unlikely that these terms are the driving mechanisms for superconductivity and ferromagnetism.

In summary, the familiar Hubbard and extended Hubbard models remain valid and useful theoretical starting points for understanding the role of e - e interactions in a variety of novel real materials.

ACKNOWLEDGMENTS

We would like to thank Dionys Baeriswyl, Sumit Mazumdar, Eugene Mele, and Alfred Zawadowski for useful discussions. We gratefully acknowledge the National Magnetic Fusion Energy Computing Center for time on CRAY computers in Livermore, California and the U.S. Department of Energy (DOE) Basic Energy Sciences Scientific Computing and Mathematical Sciences Programs.

APPENDIX A: WEAK-COUPLING PERTURBATION THEORY

We sketch here the derivation of the weak-coupling perturbation-theory expansion for the dependence at half filling of the dimerization amplitude on the e - e coupling terms.

Define the zero-order Hamiltonian, H^0 , to be $H(U=V=X=W=0)$:

$$H^0 = - \sum_{l,\sigma} (t_0 - \alpha \delta_l) (c_{l\sigma}^\dagger c_{l+1\sigma} + c_{l+1\sigma}^\dagger c_{l\sigma}) + \frac{1}{2} K \sum_l \delta_l^2 + \Gamma \sum_l \delta_l,$$

where a Lagrange multiplier term has been added to constrain the chain length. The eigenstates of H^0 for a uniform dimerization amplitude $\delta_l = (-1)^l \delta$ are well known. The zero-order ground-state wave function $|\gamma\rangle$ is just the product over occupied one-electron band states, $|k\rangle$. Define the e - e coupling terms as the perturbing Hamiltonian:

$$H^1 = U \sum_l n_{l\uparrow} + V \sum_l n_l n_{l+1} + X \sum_l B_{l,l+1} (n_l + n_{l+1}) + W \sum_l B_{l,l+1}^2.$$

When H^0 and H^1 are scaled by $H^i \rightarrow H^i / (2t_0)$, the

$$U_i([U_i] = [U, V, X, W])$$

are scaled by $U_i \rightarrow U_i / (2t_0)$, and δ is scaled by $\delta \rightarrow \alpha \delta / t_0$; all quantities depend only on the dimensionless e -ph coupling parameter $\lambda = 2\alpha^2 / \pi t_0 K$. For the rest of this Appendix, we work in these dimensionless variables.

From standard perturbation theory we can easily calculate for fixed dimerization amplitude δ the total energy $E(U, V, X, W; \delta)$ to zero, first, and second order in the e - e couplings:

$$E(U, V, X, W; \delta) \simeq E^0 + E^1 + E^2$$

where

$$E^0 = \langle \gamma | H^0 | \gamma \rangle,$$

$$E^1 = \langle \gamma | H^1 | \gamma \rangle,$$

and

$$E^2 = \sum_{\beta \neq \gamma} \frac{|\langle \gamma | H^1 | \beta \rangle|^2}{(E_\gamma - E_\beta)}.$$

The minimum-energy value δ_0 of the dimerization is found from the self-consistency equation

$$\left. \frac{\partial E}{\partial \delta} \right|_{\delta_0} = 0.$$

Defining $\delta_0 = \delta_{00}(1 + \Delta)$, where $\delta_{00} = \delta(U=V=X=W=0)$ is the self-consistent dimerization amplitude of H^0 , we can expand the self-consistency equation about δ_{00} :

$$0 \simeq \left. \frac{\partial E}{\partial \delta} \right|_{\delta_{00}} + \delta_{00} \Delta \left. \frac{\partial^2 E}{\partial \delta^2} \right|_{\delta_{00}},$$

or

$$\Delta = \frac{-1}{\delta_{00}} \left. \frac{\partial E / \partial \delta}{\partial^2 E / \partial \delta^2} \right|_{\delta_{00}}.$$

With E^0, E^1, E^2 defined as above, noting $E^0 = O(1)$, $E^1 = O(U_i)$, and $E^2 = O(U_i U_j)$, we find

$$\Delta = \frac{-1}{\delta_{00}} \left[\frac{\partial^2 E^0}{\partial \delta^2} \right]^{-1} \left[\left[\frac{\partial E^1}{\partial \delta} + \frac{\partial E^2}{\partial \delta} \right] - \left[\frac{\partial E^1}{\partial \delta} \frac{\partial^2 E^0}{\partial \delta^2} / \frac{\partial^2 E^0}{\partial \delta^2} \right] \right] \Bigg|_{\delta_{00}} + O(U_i U_j U_k)$$

$$= C_{U_i} U_i + C_{U_i, U_j} U_i U_j + O(U_i U_j U_k).$$

To find the explicit value of the C 's, we need to evaluate E^0, E^1, E^2 . Defining

$$\langle \gamma | c_{i+1\sigma}^\dagger c_{i\sigma} | \gamma \rangle = \frac{1}{2\pi\lambda} [d - (-1)^i D]$$

we obtain

$$E^0/N = \frac{1}{\pi\lambda} (-d - D\delta + \frac{1}{2}\delta^2),$$

$$E^1/N = \frac{1}{4}U + V + W - (V - 6W) \frac{(d^2 + D^2)}{2(\pi\lambda)^2} + X \frac{4d}{\pi\lambda},$$

$$E^2/N = E^{2,1}/N + E^{2,2}/N,$$

where we have introduced

$$E^{2,i} = \sum_{\beta_i \neq \gamma} \frac{|\langle \gamma | H^1 | \beta_i \rangle|^2}{(E_\gamma - E_{\beta_i})}$$

with $|\beta_1\rangle = c_{js}^\dagger c_{k\sigma} |\gamma\rangle$ and $|\beta_2\rangle = c_{js}^\dagger c_{j's'}^\dagger c_{k\sigma} c_{k'\sigma'} |\gamma\rangle$. Choosing $j' > j > k_F > k' > k$ (defining the ordering convention), we find

$$E^{2,1} = \frac{1}{N} \sum_{k, j_{\text{occ}}} \frac{-1}{|E_j| + |E_k|} \times \left\{ 8X^2 \left[\sum_n B_{kj}(n) \right]^2 + \frac{1}{2(\pi\lambda)^2} (V - 6W)^2 \left[\sum_n [d - (-1)^n D] B_{kj}(n) \right]^2 \right. \\ \left. - X(V - 6W) \frac{4}{\pi\lambda} \left[d \left[\sum_n B_{kj}(n) \right]^2 - D \sum_n B_{kj}(n) \sum_m (-1)^m B_{kj}(m) \right] \right\},$$

$$E^{2,2} = \frac{1}{N} \sum_{k, k', j, j'_{\text{occ}}} \frac{-1}{|E_j| + |E_k| + |E_{j'}| + |E_{k'}|} \\ \times [a^2 U^2 - 2abUV + \frac{1}{3}(5b^2 - 2bc)V^2 + \frac{1}{3}(b^2 - bc)(V - 6W)^2 + 4cgXV + 2g^2X^2],$$

where

$$B_{kj}(n) = (-1)^n [\psi_k(n+1)\psi_j(n) - \psi_k(n)\psi_j(n+1)],$$

$$a = \sum_n \psi_k(n)\psi_j(n)\psi_{k'}(n)\psi_{j'}(n),$$

$$b = \sum_n \psi_k(n)\psi_{k'}(n) [\psi_j(n+1)\psi_{j'}(n+1) + \psi_j(n-1)\psi_{j'}(n-1)],$$

$$c = \sum_n \psi_k(n)\psi_j(n) [\psi_{k'}(n+1)\psi_{j'}(n+1) + \psi_{k'}(n-1)\psi_{j'}(n-1)],$$

and

$$g = \sum_n [\psi_k(n+1)\psi_j(n) - \psi_k(n)\psi_j(n+1)] [\psi_{k'}(n)\psi_j(n) - \psi_{k'}(n+1)\psi_j(n+1)].$$

We have used the fact that $\psi_{j,E}(n) = (-1)^n \psi_{j,-E}(n)$ and that the ψ may be chosen real. We have evaluated the energy derivatives and finally the C 's numerically for a range of parameters; representative values are listed in Table II.

In first order, one can obtain an analytic expression for Δ . From the solutions to H^0 we have

$$d = 2\lambda \frac{(E - \delta^2 K)}{(1 - \delta^2)} \quad \text{and} \quad D = 2\delta\lambda \frac{(K - E)}{(1 - \delta^2)},$$

where E and K are the usual elliptic integrals with argument $k = (1 - \delta^2)^{1/2}$. Using the identities $\partial d / \partial \delta = -\delta \partial D / \partial \delta$ and $D|_{\delta_{00}} = \delta$ we obtain

$$\Delta^{(1)} = A \left[\frac{4\pi\lambda}{(1-d)} X + V - 6W \right] \Bigg|_{\delta_{00}},$$

where

$$A = \frac{(1-d)}{\pi\lambda} \frac{(\partial D/\partial\delta)}{[1-(\partial D/\partial\delta)]}$$

By manipulating this expression, one can show that A is positive.

APPENDIX B: NUMERICAL METHOD FOR EXACT DIAGONALIZATION

Our “exact” diagonalizations were performed using a Lanczos algorithm. We used basis states

$$c_{i_1\uparrow}^\dagger \cdots c_{i_{N_U}\uparrow}^\dagger c_{j_1\downarrow}^\dagger \cdots c_{j_{N_D}\downarrow}^\dagger |0\rangle,$$

for up electrons at sites $i_1 < i_2 < \cdots < i_{N_U}$ and down electrons at sites $j_1 < j_2 < \cdots < j_{N_D}$, where the numbers N_U and N_D of up- and down-spin fermions are both fixed and $|0\rangle$ is the vacuum state. Apart from particle-number conservation, no other symmetries were used. A new orthonormal basis was constructed by generating a sequence of states, $|\psi_1\rangle, |\psi_2\rangle, \dots$, each expressed in terms of the real-space basis. Each new state $|\psi_{n+1}\rangle$ was generated by orthogonalizing $H|\psi_n\rangle$ to $|\psi_n\rangle$ and to $|\psi_{n-1}\rangle$. This procedure generates an orthogonal set, and the Hamiltonian in this basis is tridiagonal.³⁵ Whenever generation of these new basis vectors exceeded computer memory, we diagonalized the Hamiltonian in the limited basis and resumed the generation with the eigenvector corresponding to the lowest eigenvalue as the new trial

ground-state wave function. The procedure was terminated whenever expanding the basis decreased our estimate of the ground-state energy by less than some small amount—usually 10^{-5} . The adiabatic phonons were handled by calculating the ground-state energy over a range of dimerizations and choosing the minimum-energy solution.

Our initial ground-state trial wave function was a random state, which is sure to have overlap with the true ground state for all sets of parameters. Convergence for a half-filled 8-site ring took minutes on a SUN Microsystems work station. Thereafter, using that ground state as the trial wave function for a new set of Hamiltonian parameters reduced the computer time needed for convergence from minutes to seconds—provided, of course, that the change in parameters did not take one across a “first-order phase transition:” more precisely, across a discontinuous derivative of the ground-state energy with respect to Hamiltonian parameters due to the crossing of eigenvalues. Hence, phase boundaries could be mapped quickly by running the diagonalization routine interactively—twice at once, with one job running on each side of the boundary. Each program would have to perform an expensive diagonalization starting from a random wave function only once; thereafter, one could vary parameters along the boundary smoothly for each program using the last ground state as the good guess for the new point in parameter space.

*Current address: Thinking Machines Corporation, 245 First Street, Cambridge, MA 02142-1214.

¹L. Salem, *The Molecular Orbital Theory of Conjugated Polymers* (Benjamin, New York, 1966).

²D. Baeriswyl, D. K. Campbell, and S. Mazumdar, *Theory of pi-Conjugated Polymers*, in *Conducting Polymers*, edited by H. Kiess (Springer, Heidelberg, in press).

³C. A. Coulson, Proc. R. Soc. London A **207**, 91 (1951).

⁴(a) R. G. Parr, J. Chem. Phys. **20**, 1499 (1952); (b) R. Pariser and R. G. Parr, J. Chem. Phys. **21**, 767 (1953); (c) J. A. Pople, Proc. R. Soc. London A **68**, 81 (1955).

⁵B. S. Hudson, B. E. Kohler, and K. Schulten, in *Excited States*, edited by E. C. Lin (Academic, New York, 1982), p. 1.

⁶W. P. Su, J. R. Schrieffer, and A. J. Heeger, Phys. Rev. Lett. **42**, 1698 (1979); Phys. Rev. B **22**, 2099 (1980).

⁷J. Hubbard, Proc. R. Soc. London A **276**, 238 (1963).

⁸S. Mazumdar and S. N. Dixit, Phys. Rev. Lett. **51**, 292 (1983); S. N. Dixit and S. Mazumdar, Phys. Rev. B **29**, 1824 (1984).

⁹Z. G. Zoos and S. Rameshesha, Phys. Rev. Lett. **51**, 2374 (1983).

¹⁰S. Kivelson and W. K. Wu, Phys. Rev. B **34**, 5423 (1986); W. K. Wu and S. Kivelson, *ibid.* **33**, 8546 (1986).

¹¹J. E. Hirsch, Phys. Rev. Lett. **51**, 296 (1983).

¹²S. Kivelson and D. E. Heim, Phys. Rev. B **26**, 4278 (1982)

¹³D. K. Campbell, D. Baeriswyl, and S. Mazumdar, Physica **143B**, 533 (1986).

¹⁴J. E. Hirsch and M. Grabowski, Phys. Rev. Lett. **52**, 1713 (1984).

¹⁵S. Mazumdar and S. N. Dixit, Phys. Rev. Lett. **51**, 292 (1983).

¹⁶S. Kivelson, W. P. Su, J. R. Schrieffer, and A. J. Heeger, Phys. Rev. Lett. **58**, 1899 (1987).

¹⁷In some recent physics literature, the bond-charge–bond-charge repulsion W has also been denoted by J (Ref. 21), to indicate its exchange nature, and the density-dependent hopping X by Δt (Ref. 20) or \tilde{t} (Ref. 38).

¹⁸For a complete, fairly recent discussion of what is known about the structure of polyacetylene, see J. C. W. Chien, *Polyacetylene* (Academic, New York, 1984).

¹⁹J. W. Bray, L. V. Interrante, I. S. Jacobs, and J. C. Bonner, in *Extended Linear Chain Compounds*, edited by J. S. Miller (Plenum, New York, 1983), Vol. 3, p. 355.

²⁰J. E. Hirsch, Phys. Lett. A **134**, 451 (1989); **138**, 83 (1989); Physica C **158**, 326 (1989); J. E. Hirsch and F. Marsiglio, Phys. Rev. B **39**, 11 515 (1989).

²¹J. E. Hirsch, Phys. Rev. B **40**, 2354 (1989); Phys. Rev. B (to be published); and (unpublished).

²²Basically, since the X term is not charge conjugation invariant, if it is repulsive for electrons, it is attractive for holes; this is the basis of the superconductivity arguments (Refs. 20 and 38). The exchange term W —as Heisenberg knew in 1928 [W. Heisenberg, Z. Phys. **49**, 619 (1928)]—strongly favors ferromagnetism; one sees this explicitly in our discussion of the (analytically solvable) dimer and in Ref. 21. Thus if the values of these terms can be dialed at will, one can readily explain both (electronically driven) superconductivity and ferromagnetism. However, as we argue below, one cannot choose the values of these terms independent of the values of the normal U and V ; they are all related, with the two crucial parameters determining their relations being the rate of falloff of the Wannier functions and the screening length of the “Coulomb” interaction (which screening arises from electrons

- the shape of the Wannier functions is important, different materials can have (quite) different relations among X , U , V , and W ; hence the possibility—but in our opinion not the likelihood—that these terms can explain superconductivity and ferromagnetism.
- ²³R. G. Parr, D. P. Craig, and I. G. Ross, *J. Chem. Phys.* **18**, 1561 (1950).
- ²⁴C. Wu, X. Sun, and K. Nasu, *Phys. Rev. Lett.* **59**, 831 (1987).
- ²⁵A. Painelli and A. Girlando, *Solid State Commun.* **66**, 274 (1988); *Synth. Metals* **27**, A15 (1988).
- ²⁶J. Voit, *Synth. Metals* **27**, A33-A40 (1988); *Phys. Rev. Lett.* **64**, 323 (1990); in *Proceedings of the NATO Advanced Research Workshop on Interacting Electrons in Reduced Dimensions*, edited by D. Baeriswyl and D. K. Campbell (Plenum, New York, in press).
- ²⁷J. Tinka Gammel and D. K. Campbell, *Phys. Rev. Lett.* **60**, 71 (1988) (C); D. K. Campbell, J. Tinka Gammel, and E. Y. Loh, Jr., *Phys. Rev. B* **38**, 12043 (1988); *Synth. Metals* **27**, A9 (1988); in *Proceedings of the NATO Advanced Research Workshop on Interacting Electrons in Reduced Dimensions*, edited by D. Baeriswyl and D. K. Campbell (Plenum, New York, in press).
- ²⁸This is the same as Ref. 16 for $X=0$; note that there is a factor of 2 difference in our definitions of W .
- ²⁹J. Solyom, *Adv. Phys.* **28**, 201 (1979).
- ³⁰V. J. Emory, in *Highly Conducting One-Dimensional Solids*, edited by J. T. DeVreese, R. P. Evrard, and V. E. van Doren (Plenum, New York, 1979), p. 247.
- ³¹(a) J. C. Bonner and M. E. Fisher, *Phys. Rev.* **135**, A640 (1964); (b) R. L. Orbach, *ibid.* **112**, 309 (1958).
- ³²Here in view of the later comparisons to intermediate coupling, we keep the correction to Δ due to V but ignore a (smaller, for the range of values considered) correction due to W . As $U \rightarrow \infty$, all these corrections are of course higher order.
- ³³This is the important sense in which W differs from the simple hopping term, t_0 , which leads to hybridization and a lowering of the energy.
- ³⁴E. Fradkin and J. E. Hirsch, *Phys. Rev. B* **27**, 1680 (1983); J. E. Hirsch and E. Fradkin, *Phys. Rev. Lett.* **49**, 402 (1982).
- ³⁵See, e.g., the section on Lanczos diagonalization in S. Pissanetsky, *Sparse Matrix Technology* (Academic, London, 1984).
- ³⁶(a) A. J. Heeger and J. R. Schrieffer, *Solid State Commun.* **48**, 207 (1983); (b) H. Thomann, L. R. Dalton, M. Grabowski, and T. C. Clarke, *Phys. Rev. B* **31**, 3141 (1985).
- ³⁷K. Fesser, A. R. Bishop, and D. K. Campbell, *Phys. Rev. B* **27**, 4804 (1983).
- ³⁸A. Zawadowski, *Phys. Rev. B* **39**, 4682 (1989).
- ³⁹D. Baeriswyl and K. Maki, *Mol. Cryst. Liq. Cryst.* **118**, 1 (1985).